

Original Article

Combined effect of phase change material and fluid flow
on solar thermal energy storageThanwit Naemsai^{1*}, Jaruwat Jareanjit¹, and Kunlapat Thongkaew²¹ Department of Mechanical Engineering, Faculty of Engineering,
Rajamangala University of Technology Srivijaya, Mueang, Songkhla, 90000 Thailand² Department of Industrial Engineering, Faculty of Engineering,
Prince of Songkhla University, Hat Yai, Songkhla, 90110 Thailand

Received: 30 March 2020; Revised: 8 June 2020; Accepted: 5 July 2020

Abstract

The combined effect of phase change material (PCM) and fluid flow on the thermal efficiency of solar thermal storage was experimentally investigated in this study in order to determine the appropriate operating conditions. Moreover, a sensitivity analysis was employed to evaluate the greatest effect on thermal efficiency. In the experiments, the effect of PCM weight was tested with three values of 4, 6, and 8 kg. The effect of fluid flow rate was also examined with three values of 2.4, 4.8, and 7.2 L/min. From the experiment, PCM and fluid flow had a significant effect on thermal efficiency. In the case of optimal conditions, the PCM of 6 kg and flow rate of 4.8 L/min provided the water and air heating efficiencies of 65% and 45%, respectively. From the sensitivity analysis, PCM showed the greatest effect on thermal efficiency, leading to a priority factor for solar thermal storage design.

Keywords: combined effect, phase change material, fluid flow, solar energy, thermal storage

1. Introduction

Solar energy, which provides a clean and renewable source of power, can be used to sustainably fulfill global energy needs. Sustainable energy technologies are essential to implement for future energy needs because these technologies guarantee a non-stop supply of energy. Solutions for sustainable energy technologies comprise effective utilization, conversion, and storage (Sajawal *et al.*, 2019). The most common solar-thermal applications used in residences and industries are water heaters (Fazilati & Alemrajabi, 2013; Hashim *et al.*, 2018; Mandal & Ghosh, 2020) and air heaters (Abuşka, Şevik, & Kayapınar, 2019; Kabeel, Khalil, Shalaby, & Zayed, 2016; Poblete & Painemal, 2020). However, one challenge facing the widespread usage of solar energy is reduced or curtailed energy production during cloudy or foggy weather and the lack of solar production at night. Thus,

thermal energy storage with phase change material (PCM), an effective sustainable energy technique, can provide a workable solution to this challenge (Kee, Munusamy, & Ong, 2018).

Many previous studies have investigated the addition of PCMs to increase the efficiency of thermal energy storage. Fazilati and Alemrajabi (2013) presented the effect of PCM on the performance of a solar water heater. It was found that the energy storage density in the tank increased by up to 39% and it could supply hot water with a specified temperature for a 25% longer time period. After that, Kee *et al.* (2018) proposed solar water heaters incorporating solid-liquid organic PCMs as thermal storage. It was noted that the suitable phase change temperature for the solar water heater was in the range of 40–70 °C. Apart from the addition of PCM in a solar water heater, the effect of fluid flow on the thermal performance has been also investigated. Hussain and Lee (2014) investigated the thermal efficiency of the conical solar water heater with an attached thermal storage tank, which was increased by an increase in flow rate. The maximum efficiency was obtained at a critical flow rate of 6 L/min.

*Corresponding author

Email address: thanwit.n@rmutsv.ac.th

Further, the efficiency began to decrease when the flow rate increased beyond this critical value. These results were similar to the effect of the mass flow rate on the thermal efficiency of the flat plate solar water heating system with nanofluid (Prakasam, Vellingiri, & Nataraj, 2017). Recently, Mandal and Ghosh (2020) studied the thermal performance of a double-pass solar water heater with reflector; it was observed that the thermal efficiency for high mass flow rates was slightly different.

For solar air heater applications, Kabeel *et al.* (2016) proposed a solar heater using PCM was 12% higher than the corresponding ones without using PCM. The convective heat transfer coefficient of the flat plate solar air heater increased as the mass flow increased. Abuşka *et al.* (2019) studied the effect of using PCM and honeycomb on thermal efficiency. The average day-time thermal efficiency of the heaters with PCM increased for the low mass flow rates. Afterward, it decreased for the higher mass flow rates. These results were in accordance with the data found in the solar water heater (Hussain & Lee, 2014; Prakasam *et al.*, 2017). Moreover, numerical simulation was employed to describe the PCM charging and discharging process inside the storage tank. It can be concluded that the thermal efficiency was dependent on the air mass flow rate and the amount of PCM (Bouhal, El Rhafikic, Kousksoub, Jamila, & Zeraouli, 2018; Moradi, Kianifar, & Wongwises, 2017).

As mentioned above, although some publications have reported on the effects of PCM quantity added and flow fluid on thermal efficiency, few studies are available concerning the thermal efficiency of solar air and water heaters with thermal storage considering the combined effect of PCM quantity added and flow fluid. Furthermore, the parametric sensitivity analysis of both effects on thermal efficiency has yet to be reported. Thus, in order to clarify and resolve the aforementioned challenging issues, the purpose of the present work is to experimentally investigate the effects of PCM quantity added and fluid flow on the thermal efficiency. Furthermore, parametric sensitivity analysis of both effects on thermal efficiency was also evaluated. This guideline is expected to be beneficial for solar thermal storage design and efficient operation.

2. Materials and Methods

2.1 Experimental setup and procedure

The experiment was carried out at Rajamangala University of Technology Srivijaya, Songkhla, Thailand (7.078 °N and 100.597 °E, respectively). The experimental setup consisted of a flat plate solar collector, a controller, a hot-air heat exchanger, a 20-liter water tank with a water pump, and a PCM tank, as displayed in Figure 1(a). A flat plate solar collector with a gross area of 2.5 m² was installed at an inclination of 7° south-facing slope. The efficiency of the solar collector was evaluated by ANSI/ASHRAE STANDARD 93-2003 coded “86244 PC 5/03” (Ashrae, 1989), which was approximately 72%. The hot water heat exchanger tank was made of a stainless sheet of 0.8 mm and 7 m copper coil was attached circumferentially inside the water tank. PCM was encapsulated in a cylindrical container because it is an easy geometric configuration for the manufacturing process and the quality of the thermal

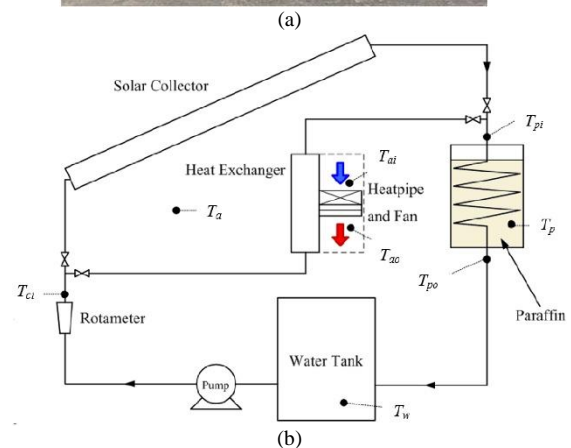


Figure 1. Solar thermal energy storage: (a) experimental setup; (b) diagram of temperature positioning

transferring surface between the circulating water and the PCM (Gautam & Saini, 2020). Moreover, the heat pipe thermal module was applied in the apparatus as the hot-air heat exchanger because heat pipes not only effectively transfer heat between two solid interfaces, but also exert a better strengthening effect on phase-change heat storage than conventional heating methods (Wang *et al.*, 2019). A galvanized sheet was used to fabricate the body of the storage and water tanks, in which glass wool with a thickness of 2 cm was used as the insulator.

In the experiment, the effect of PCM quantity added was tested at three levels including 4, 6, and 8 kg. The effect of fluid flow was also examined with three volumetric flow rates of 2.4, 4.8, and 7.2 L/min. These fluid flow rates were set by ANSI/ASHRAE STANDARD 93-2003 (Ashrae, 1989). All tests were initiated from 9.00 a.m. to 8.00 p.m. (i.e. operating time of 11 hr) and the water flow rate was set at the specific value of each PCM weight. However, the fluid flow circulating system was started at 10 a.m. because the PCM needed to be preheated to nearly melting temperature. Fully refined paraffin wax was used as PCM, in which the properties includes 55–60 °C melting temperature, 2.14 kJ/kg K specific heat capacity and 0.2 W/m K heat conductivity (ExxonMobil Waxes, 2020). The data acquisition modules consisted of a temperature recorder (Yokogawa MV200 datalogger) connected with 8 points of Chromel-Alumel thermocouple (type K), an anemometer (Osman smart sensor AR866A), a rotameter (Nitto VA10S-15) and a Pyranometer (Modbus protocol SR20-D1). The function of the Osman anemometer is for recording air velocity, whereas the Nitto

rotameter and the Modbus Pyranometer are for recording water flow rate and solar radiation, respectively. Thermal acquisition was evaluated from the eight locations, including ambient temperature (T_{am}), PCM temperature (T_p), the inlet temperature of PCM tank (T_{pi}), the outlet temperature of PCM tank (T_{po}), hot water temperature (T_w), the inlet temperature of the solar collector (T_{ci}), the inlet temperature of an air heater (T_{ai}) and outlet temperature of an air heater (T_{ao}), as shown in Figure 1(b).

All experiments were replicated three times and the uncertainties of parameters throughout the solar thermal heat storage were taken as the final data, as depicted in Table 1. The uncertainties of independent variables (w_1, w_2, \dots, w_n) were assessed to define the total uncertainty (W_R), as Equation 1 (Sevik, 2014). Where, x_1, x_2, \dots, x_n were independent variables.

$$W_R = \left[\left(\frac{\partial R}{\partial x_1} w_1 \right)^2 + \left(\frac{\partial R}{\partial x_2} w_2 \right)^2 + \dots + \left(\frac{\partial R}{\partial x_n} w_n \right)^2 \right]^{1/2} \quad (1)$$

Table 1. Uncertainties of parameters throughout solar thermal storage

Parameters	Uncertainty	Unit
Temperature	±0.5	°C
Water flow rate	±0.1	L/min
Solar radiation	±1.0	W/m ²
Time measurement	±0.1	min
Air velocity	±0.1	m/s

2.2 Thermal performance analysis

Thermal efficiency was employed to indicate the thermal performance because of a dimensionless analysis that can be further compared to the performance with other systems (Hussain & Lee, 2014; Wang *et al.*, 2019). According to the performance analysis, thermal efficiency can be divided into two cases: water heating efficiency and air heating efficiency. Efficiencies were evaluated particularly at the operating time from 12:00 p.m. to 8:00 p.m due to the discharge mode of PCM. The average thermal efficiency can be calculated by equation (2) as:

$$\eta_{avg} = \frac{\eta_{thw} + \eta_{tha}}{2} \quad (2)$$

where η_{thw} is the water heating efficiency and η_{tha} is the air heating efficiency. The value of water heating efficiency (η_{thw}) and air heating efficiency (η_{tha}) can be calculated as:

$$\eta_{thw} = \frac{\dot{m}_w C_p (T_{po} - T_{pi})}{GA_c} \quad (3)$$

$$\eta_{tha} = \frac{\dot{m}_a C_p (T_{ao} - T_{ai})}{GA_c} \quad (4)$$

where, m is mass flow rate, C_p is specific heating capacity, A_c is absorbed thermal area and G is solar radiation.

For the analysis of the optimal operating condition for thermal storage, a non-dimensional level variable was employed. Variables of fluid flow ratio and PCM ratio were used in order to simplify parameterized problems. The fluid flow ratio (q^*) and the adding PCM ratio (m^*) can be calculated from Equations 5 and 6, respectively, as

$$q^* = \frac{q}{q_{max}} \quad (5)$$

$$m^* = \frac{m_{pcm}}{m_{max}} \quad (6)$$

where q is the tested flow rate, q_{max} is the maximum flow rate, m_{pcm} is the adding PCM mass, and m_{max} is the maximum PCM mass contained inside the tank.

Sensitivity analysis was also employed to determine the greatest effect of solar thermal storage on thermal efficiency. A simple method for determining parameter sensitivity is the sensitivity index (SI) that is introduced by Hoffman and Gardner (1983). The SI is generally used to calculate the output percent difference when varying one input parameter from its minimum value (x_{min}) to its maximum value (x_{max}), as shown in Equation 7.

$$SI = \frac{x_{max} - x_{min}}{x_{max}} \times 100 \quad (7)$$

3. Results and Discussion

The air and water heating efficiencies of the thermal heat storage assisting with the flat plate solar collector were investigated with different ranges of volumetric flow rates and PCM weights. All experiments were conducted on consecutive clear-sky days in April 2019. For the clear sky condition, the solar radiation of each experiment had a slight difference. It can be concluded that various solar conditions and ambient temperature barely affected the thermal efficiency of the PCM storage system (Hussain & Lee, 2014; Wang *et al.*, 2019). The effects of PCM quantity and fluid flow are discussed in this section. Furthermore, the thermal sensitivity of PCM quantity and fluid flow was also evaluated to determine the greatest effect on the thermal efficiency of solar thermal storage.

3.1 Effect of PCM addition

Solar radiation depends mainly on location and local weather. Experiments of adding the PCM effect were performed over three days (from 6th to 8th April 2019) with mostly clear sky conditions. In the experiments, hot water and air temperatures were tested under the condition of the flat plate arrangement and a flow rate of 4.8 L/min. Under these conditions, the PCM weights were varied at 4, 6, and 8 kg. The water and air temperatures were proportional to the solar radiations, as displayed in Figure 2. It was observed that the maximum water and temperature appeared at the operating time around 6 hr. After that, the water temperature dropped steadily when solar radiation decreased. At nighttime, the highest temperature appeared at the condition of 8 kg PCM

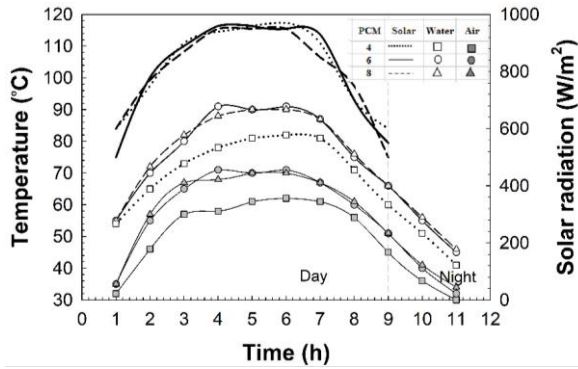


Figure 2. Hourly distribution of water and air temperatures at different PCM weights

because of the higher latent heat from the larger mass. Additionally, it was noted that the use of paraffin in the PCM tank could extend the time of hot water provision over 40 °C when the PCM released large amounts of thermal energy at a relatively constant temperature under the discharging mode (Fazilati & Alemrajabi, 2013). For the heating air system, the air temperatures were similar to the water temperatures. The highest temperature also appeared at the condition of 8 kg PCM. Moreover, the temperature difference between water and air was around 20 °C due to the physical properties of matter.

The effect of PCM quantity added on the thermal efficiency of the solar water heater was compared with the relevant work of Bouhal *et al.* (2018). Normalized values were used to analyze the effect of adding PCM on thermal efficiency, as shown in Figure 3. Normalized values for thermal efficiency ($\eta_{thw} / \eta_{thw} @ m_{PCM_max}$) were calculated from the efficiencies at the reference points (maximum adding PCM), as listed in Table 2. In addition, reference points were given by the points of the highest thermal efficiency. It was noticed from Figure 3 that the adding PCM increased with an increase the thermal efficiency. These trends seem to be in accordance with previous work (Bouhal *et al.*, 2018). It was indicated that the sensible heat through the PCM tank depended on the mass of adding PCM during the discharging mode. Hence, the PCM quantity added to the thermal heat storage greatly affected its thermal efficiency.

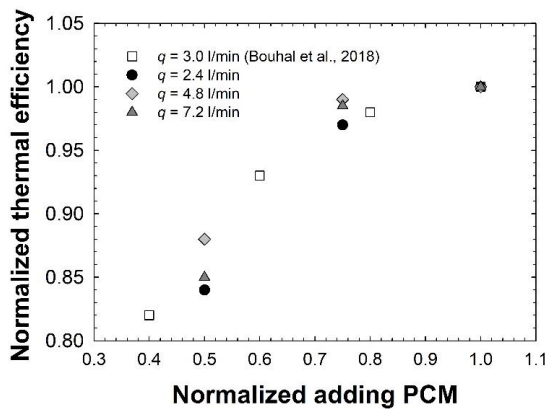


Figure 3. Effect of the normalized adding PCM on thermal efficiency

Table 2. Thermal efficiencies of solar water heater at reference points (m_{PCM_max})

Reference	Flow rate (L/min)	PCM weight (kg)	Thermal efficiency (%)
This study	2.4	8.0	58.3
	4.8	8.0	66.9
	7.2	8.0	66.8
Bouhal <i>et al.</i> (2018)	3.0	6.5	66.1

3.2 Effect of fluid flow

The hourly change of the solar radiation from 10th to 12th April 2019 and the hourly distribution of water and air temperatures are depicted in Figure 4. The adding PCM was controlled at 6 kg, whereas the flow rates were ranged at 2.4, 4.8, and 7.2 L/min, respectively. It was clear that the air and water temperatures were directly altered by solar radiation. At the specific operating time during daytime, the water temperatures at the higher flow rate became higher than that of the lower flow rate. These results were similar to previous work (Hussain & Lee, 2014). Moreover, it was observed that the water temperatures between flow rates of 4.8 and 7.2 L/min were slightly different during the daytime because PCM had a nearly constant value and was slightly dependent on the high flow rate during the discharging mode (Moradi *et al.*, 2017). However, the highest water temperature at nighttime appeared in the case of a flow rate of 4.8 L/min. It was implied that this flow rate was able to offer better latent heat changing in the PCM phase to the sensible heat of water flowing through the PCM tank than the others. Furthermore, these results of water temperature were in accordance with the experimental results of the air temperatures. It was found that the highest temperature appeared at the condition of 4.8 L/min flow rate.

The effect of fluid flow on the thermal efficiency of the solar water heater was compared with previous work (Mandal & Ghosh, 2020). The effect of fluid flow on the thermal efficiency was present in terms of normalized values to analyze the characteristics of quality information, as shown in Figure 5. The normalized values for thermal efficiency ($\eta_{thw} / \eta_{thw} @ q_max$) were calculated from the efficiencies at the reference points, as exhibited in Table 3. It was found that the fluid flow had a significant effect on thermal efficiency; thermal efficiency increased when the flow rate increased. These trends also corresponded to the work of Mandal and Ghosh (2020). The main reason was that the heat transfer rate was proportional to the flow rate through the PCM tank.

3.3 Combined effect of PCM quantity added and fluid flow

In this section, the combined effect of the fluid flow rate and PCM quantity added on thermal efficiency is presented and shown in Figure 6. As a result, thermal efficiency was directly dependent upon both effects. The thermal efficiency (η_{avg}) of the solar thermal storage can be calculated from the average water heating and air heating efficiencies (Equation 4). The three-dimensional curvature (3D), which was useful for establishing desirable response

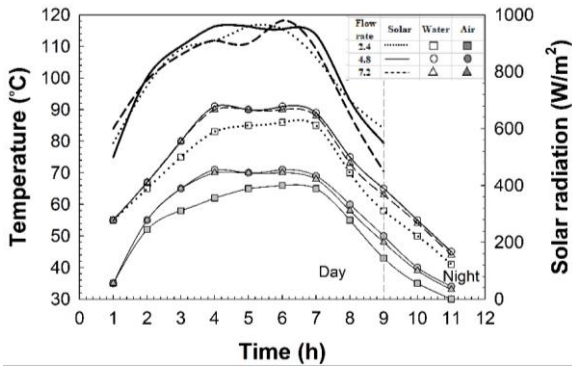


Figure 4. Hourly distribution of water and air temperatures at different flow rates

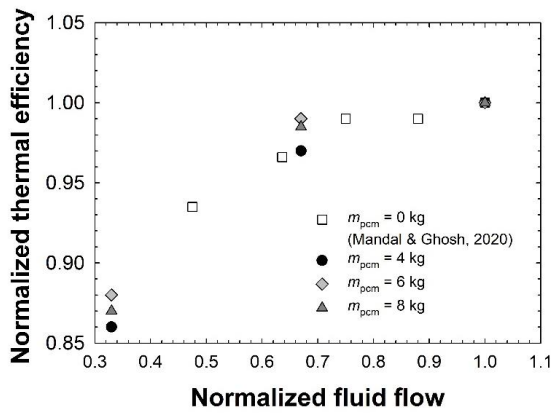


Figure 5. Effect of the normalized fluid flow on thermal efficiency

Table 3. Thermal efficiencies of solar water heater at reference points (q_{max})

Reference	Flow rate (L/min)	PCM weight (kg)	Thermal efficiency (%)
This study	7.2	4.0	57.2
	7.2	6.0	65.2
	7.2	8.0	65.8
Mandal and Ghosh (2020)	4.0	0.0	50.3

values and operating conditions, was employed to describe the combined effects in order to determine the appropriate operating conditions for solar thermal storage.

Both, fluid flow and adding PCM were set in terms of dimensionless parameters, which can be calculated from Equations (5) and (6). The scope of this study should be identified by flow rate ratio, q^* , of 0.33, 0.66 and 1.00; and PCM ratio, m^* , of 0.4, 0.6, and 0.8. From Figure 6, high values of thermal efficiency appeared under the operating conditions of 0.66-1.00 fluid flow ratio and 0.6-0.8 adding PCM ratio. The lowest thermal efficiency emerged at the fluid flow ratio of 0.33 and the adding PCM ratio of 0.4. It can be seen that the combined effects directly superimposed the thermal efficiency. Furthermore, the higher PCM ratio could compensate for the effect of the low flow rate ratio on thermal efficiency. Otherwise, the operating conditions of the solar

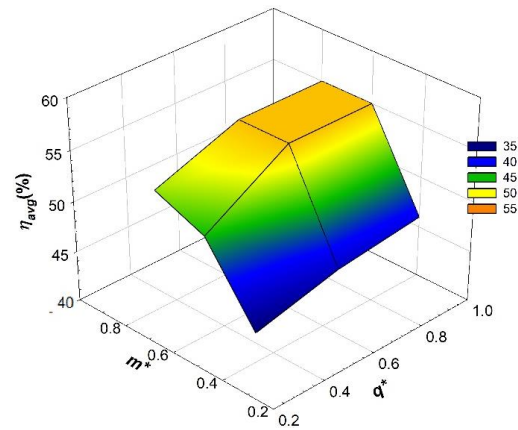


Figure 6. Combined effect of fluid flow and PCM on thermal efficiency

thermal storage had a good tradeoff between the higher PCM ratio and the lower fluid flow ratio. For the appropriate operating condition, the surface plot can be determined by solar thermal storage with the highest average thermal efficiency of 55%. It can be concluded that the appropriate operating condition included the adding PCM ratio of 0.6 (i.e. 6 kg) and a fluid flow ratio of 0.66 (i.e. 4.8 L/min). These conditions could save on both installation and operating costs when compared with the operating condition with PCM of 8 kg and a fluid flow rate of 7.2 L/min under the same average thermal efficiency.

It was also observed that thermal efficiency increased by approximately 30% when the PCM ratio increased from 0.4 to 0.6 at the same fluid flow ratio of 0.66. At the PCM ratio of 0.6, thermal efficiency increased by only 23% when the fluid flow ratio increased from 0.33 to 0.66. Nevertheless, it was somewhat difficult to select the greatest effect between the fluid flow rate and the adding PCM on thermal efficiency. Therefore, sensitivity analysis using the SI method of both effects was essential for this study.

In the SI analysis, the thermal storage operation with a PCM weight of 4 kg and a flow rate of 2.4 L/min was set as a reference point to calculate the SI. In addition, the average thermal efficiency of the solar thermal storage at the reference point was 43.5%. The varied inputs of adding PCM and fluid flow were expressed as the percentage of changing effect. The percentages of PCM and fluid flow determined by the SI method were 50.00% and 66.67%, respectively. The percentages of changing thermal efficiencies at different changing effects are depicted in Figure 7. It was noted that the operating conditions for solar thermal storage designed by the increase in PCM mass had a more significant effect on average thermal efficiency than that of operating conditions with an increase in fluid flow rate approximately 29% from the SI slope of 0.17. Moreover, the results of the sensitivity analysis corresponded to the results analyzed by the surface plot, as shown in Figure 6.

The effect of the PCM quantity added can be a priority for solar thermal storage design. It was inferred that the latent heat obtained by the PCM quantity added had a higher effect on heat and mass transfer of the solar thermal storage than the sensible heat determined by the mass flow rate through the PCM tank. By comparison, the thermal

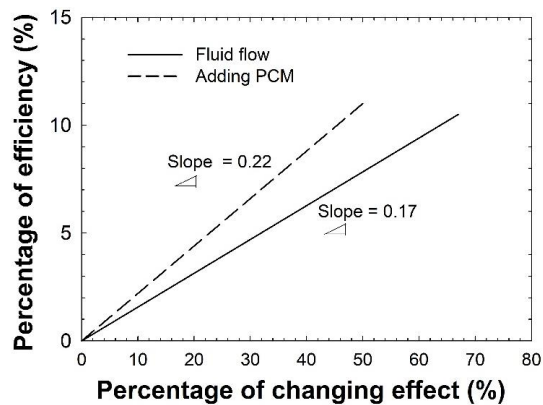


Figure 7. Sensitivity index of the thermal efficiency

efficiency with previous works, in the case of the solar water heater (Hashim *et al.*, 2018; Mandal & Ghosh, 2020; Wang *et al.*, 2019), showed that this study provided a thermal efficiency of 65.0 %, which was slightly higher than others. On the other hand, the thermal efficiency of the solar air heater in this study was 45%, lower than in previous works (Kabeel *et al.*, 2016; Sajawal *et al.*, 2019) because of the different solar heating utilizations. Therefore, solar thermal energy storage will be examined further in future work using a larger-scale solar water and air heating application.

4. Conclusions

The solar thermal storage integrated with PCM (paraffin wax) was designed to exploit the water and air heater application. The combined effect of fluid flow and PCM quantity added was experimentally investigated in order to determine the appropriate operating conditions for solar thermal storage. In addition, parametric sensitivity analysis was discussed to obtain the greatest significant effect on thermal efficiency. From the experimental results, the PCM quantity added significantly affected thermal efficiency, in which an increase in the PCM quantity increased the thermal efficiency. However, the efficiency remained constant when the PCM quantity added was higher than 6 kg because of the thermal equilibrium state. Thermal efficiency was also significantly induced by the fluid flow, where the fluid flow rate of 7.2 L/min had better thermal efficiency than the others because of the sensible heat. In terms of sensitivity analysis, the PCM quantity had the greatest effect on thermal efficiency. In addition, a proper selection of both the PCM quantity and the fluid flow rate could greatly superimpose the thermal efficiency of solar thermal storage. The recommendation for optimal conditions is the PCM quantity added of 6 kg and a fluid flow rate of 4.8 L/min. This results in solar thermal storage providing water and air heating efficiency of 65% and 45%, respectively.

Acknowledgements

This research was supported by Department of Mechanical Engineering, Faculty of Engineering, Rajamangala University of Technology Srivijaya for the financial support.

References

- Abuşka, M., Şevik, S. & Kayapınar, A. (2019). A comparative investigation of the effect of honeycomb core on the latent heat storage with PCM in solar air heater. *Applied Thermal Engineering*, 148, 684-693. Retrieved from <https://www.sciencedirect.com/science/article/pii/S1359431118328497>
- Ashrae, (1989). *ANSI/ASHRAE 96-1980 (RA 1989)— Methods of testing to determine the thermal performance of unglazed flat-plate liquid-type solar collectors*. Retrieved from <https://webstore.ansi.org/standards/ashrae/ansiashrae961980ra1989>
- Bouhal, T., El Rhafikic, T., Kousksoub, T., Jamila, A. & Zeraouli, Y. (2018). PCM addition inside solar water heaters: Numerical comparative approach. *Journal of Energy Storage*, 19, 232–246. Retrieved from <https://www.sciencedirect.com/science/article/pii/S2352152X18304134>
- ExxonMobil Waxes. (2020). Parvan™ – Fully refined paraffin wax. Retrieved from <https://www.exxonmobil.com/en/wax/fully-refined-paraffin-wax>
- Fazilati, M. A. & Alemrajabi, A. A. (2013). Phase change material for enhancing solar water heater, an experimental approach. *Energy Conversion and Management*, 71, 138-145. Retrieved from <https://www.sciencedirect.com/science/article/pii/S0196890413001775>
- Gautam, A. & Saini, R. P. (2020). A review on technical, applications and economic aspect of packed bed solar thermal energy storage system. *Journal of Energy Storage*, 27, 101046. Retrieved from <https://www.sciencedirect.com/science/article/pii/S2352152X19309533>
- Hashim, W. M., Shomran, A. T., Jurmut, H. A., Gaaz, T. S., Kadhun, A. A. & Al-Amiery, A. A. (2018). Case study on solar water heating for flat plate collector. *Case Studies in Thermal Engineering*, 12, 666-671. Retrieved from <https://www.sciencedirect.com/science/article/pii/S2214157X18301771>
- Hoffman, F. O. & Gardner, R. H. (1983). Evaluation of uncertainties in environmental radiological assessment models. In J. E. Till & H. R. Meyer (Eds.), *Radiological assessments: a textbook on environmental dose assessment, Report No. NUREG/CR-3332*. Washington, DC: U.S. Nuclear Regulatory Commission.
- Hussain, M. I. & Lee, G. H. (2014). Thermal performance evaluation of a conical solar water heater integrated with a thermal storage system. *Energy Conversion and Management*, 87, 267–273. Retrieved from <https://www.sciencedirect.com/science/article/pii/S0196890414006542>
- Kabeel, A. E., Khalil, A., Shalaby, S. M. & Zayed, M. E. (2016). Experimental investigation of thermal performance of flat and v-corrugated plate solar air heaters with and without PCM as thermal energy storage. *Energy Conversion and Management*, 113, 264-272. Retrieved from <https://www.sciencedirect.com/science/article/pii/S0196890416300127>

- Kee, S. Y., Munusamy, Y. & Ong, K. S. (2018). Review of solar water heaters incorporating solid-liquid organic phase change materials as thermal storage. *Applied Thermal Engineering*, 131, 455-471. Retrieved from <https://www.sciencedirect.com/science/article/pii/S1359431117347804>
- Mandal, S. & Ghosh, S. K. (2020). Experimental investigation of the performance of a double pass solar water heater with reflector. *Renewable Energy*, 149, 631-640. Retrieved from <https://www.sciencedirect.com/science/article/pii/S0960148119318695>
- Moradi, A., Kianifar, A. & Wongwises, S. (2017). Optimization of a solar air heater with phase change materials: Experimental and numerical study. *Experimental Thermal and Fluid Science*, 89, 41-49. Retrieved from <https://www.sciencedirect.com/science/article/pii/S0894177717302078>
- Prakasam, M. J., Vellingiri, A. T. & Nataraj, S. (2017). An experimental study of the mass flow rates effect on flat-plate solar water heater performance using Al₂O₃/Water nanofluid. *Thermal Sciences*, 21, S379-S388. Retrieved from <https://pdfs.semanticscholar.org/9b05/2de02c52b2f7953b123d8e56c7a8a883d03b.pdf>
- Poblete, R. & Painemal, O. (2020). Improvement of the solar drying process of sludge using thermal storage. *Journal of Environmental Management*, 255, 109883. Retrieved from <https://www.sciencedirect.com/science/article/pii/S0301479719316019>
- Sajawal, M. Rehman, T., Ali, H. M., Sajjad, U., Raza, A. & Bhatti, M. S. (2019). Experimental thermal performance analysis of finned tube-phase change material based double pass solar air heater. *Case Studies in Thermal Engineering*, 15, 100543. Retrieved from <https://www.sciencedirect.com/science/article/pii/S2214157X19301480>
- Sevik, S. (2014). Experimental investigation of a new design solar-heat pump dryer under the different climatic conditions and drying behavior of selected products. *Solar Energy*, 105, 190–205. Retrieved from <https://www.sciencedirect.com/science/article/abs/pii/S0038092X14001716>
- Wang, Z., Diao, Y., Zhao, Y., Yin, L., Chen, Ch., Liang, Lin & Wang, T. (2019). Performance investigation of an integrated collector-storage solar water heater based on lap-joint-type micro-heat pipe arrays, *Applied Thermal Engineering*, 153, 808–827. Retrieved from <https://www.sciencedirect.com/science/article/pii/S1359431118362884>